Biological Activity and Ferric Ion Binding of Fragments of Glycine-Extended Gastrin†

Hong He,‡ B. Philip Shehan,‡ Kevin J. Barnham,§ Raymond S. Norton,|| Arthur Shulkes,‡ and Graham S. Baldwin*,‡

The University of Melbourne Department of Surgery, Austin Health, Heidelberg, Victoria 3084, Australia, The University of Melbourne Department of Pathology and The Mental Health Research Institute of Victoria, Parkville, Victoria 3010, Australia, and The Walter and Eliza Hall Institute of Medical Research, 1G Royal Parade, Victoria 3050, Australia

Received February 26, 2004; Revised Manuscript Received June 28, 2004

ABSTRACT: Nonamidated gastrins such as progastrin and glycine-extended gastrin17 (Ggly) induce cell proliferation and migration in vitro and colonic mucosal proliferation in vivo. Our earlier NMR study defined the structure of Ggly and showed that ferric ions are essential to its biological activity, with the first binding to Glu7 and the second to Glu8 and Glu9 (Pannequin, J. et al. (2002) *J. Biol. Chem. 277*, 48602−48609). The aims of this study were to define the minimum biologically active fragment of Ggly and to determine whether ferric ions were also required for its activity. Cell-proliferation studies with Ggly fragments containing the five glutamate residues showed that the nonapeptide LE_5AYG, the octapeptide LE_5AY, and the heptapeptides E_5AY and LE_5A were fully active and that their activity was dependent on the presence of ferric ions. The activity of the hexapeptides LE_5 and E_5A and the pentapeptide E_5 was reduced and independent of the presence of iron. The stoichiometry of ferric ion binding to LE_5AYG, LE_5AY, and E_5AY, determined by absorption spectroscopy, was 2 mol/mol. NMR spectroscopy showed that the nonapeptide LE_5AYG and shorter fragments had no defined structure and that the iron-binding sites differed from those in Ggly. We conclude that, in contrast to amidated gastrins where the C-terminal tetrapeptide is the minimum bioactive fragment, the shortest fully active fragments of Ggly are the heptapeptides LE_5A and E_5AY. These observations indicate that extensive proteolytic processing may not completely inactivate Ggly and that bioactive forms that are not detected by current radioimmunoassays may be present in tissues and/or plasma.

The 80-residue prohormone progastrin is produced by G cells located within the gastric antrum and is processed to shorter peptides, such as the 18-residue peptide glycine-extended gastrin (Ggly)[1] and amidated gastrin17 (Gamide) (Figure 1) (*1*). Until recently, amidation of the carboxy terminus of gastrin was thought to be essential for biological activity (*2*). However, we and others have reported that Ggly and progastrin are able to induce proliferation and migration of various cell lines in vitro (*3*−*7*) and proliferation of the colonic mucosa in vivo (*8*−*10*). In addition, Ggly acts synergistically with Gamide in the stimulation and maintenance of elevated gastric acid production (*11*, *12*).

	1 6 7 8 9 10 18
Ggly	Z G P W L E E E E E A Y G W M D F G OH
Ggly1-11	Z G P W L E E E E E A OH
Ggly5-18	L E E E E E A Y G W M D F G OH
Ggly5-13	L E E E E E A Y G OH
Ggly5-12	L E E E E E A Y OH
Ggly5-11	L E E E E E A OH
Ggly5-10	L E E E E E OH
Ggly6-12	E E E E E A Y OH
Ggly6-11	E E E E E A OH
Ggly6-10	E E E E E OH

FIGURE 1: Sequences of human Ggly (Ggly1−18) and related peptides. Amino acids are shown in the one letter code, where Z represents a pyroglutamate residue. Ggly corresponds to residues 55−72 of $progastrin_{1-80}$.

A mixture of shorter forms of Gamide, including amidated gastrin 2−17, 4−17, 6−17, and 13−17, has been found in the antrum and circulation (*13*, *14*). The occurrence of C-terminal fragments of nonamidated gastrins shorter than Ggly has not been investigated, but N-terminal fragments,

† This work was supported by Grant A00103736 (to G.S.B. and R.N.) from the Australian Research Council, Grants 980625 (to G.S.B.), 208926 (to G.S.B.) and 114123 (to A.S.) from the National Health and Medical Research Council of Australia, Grant GM65926-01 (to G.S.B., R.N., and A.S.) from the National Institutes of Health, and by the Austin Hospital Medical Research Foundation (to G.S.B. and A.S.).

* To whom correspondence should be addressed: Department of Surgery, Austin Health, Studley Road, Heidelberg, Victoria 3084, Australia. Telephone: 613-9496-5592. Fax: 613-9458-1650. E-mail: grahamsb@unimelb.edu.au.

‡ The University of Melbourne Department of Surgery, Austin Health.

§ The University of Melbourne Department of Pathology.

|| The Walter and Eliza Hall Institute of Medical Research.

[1] Abbreviations: CTFP, C-terminal flanking peptide of progastrin; DMEM, Dulbecco's modified Eagle's medium; FBS, fetal bovine serum, Gamide, amidated gastrin17; Ggly, glycine-extended gastrin17; ED_{50}, concentration required for 50% stimulation; K_d, dissociation constant; NMR, nuclear magnetic resonance.

10.1021/bi0495984 CCC: $27.50
Published on Web 08/27/2004

particularly gastrin1−10, are also present (*14*). The formation of the gastrin heptapeptide E_5AY and similar fragments may be inferred from different combinations of the cleavages that generated the above fragments. However, because of a lack of suitable antisera, processed gastrins lacking both the N and C terminus of Gamide have not been detected to date. The formation of gastrin fragments shorter than 17 residues may also be inferred from the observation that in human antrum the concentration of the C-terminal flanking peptide of progastrin (CTFP) is about 40% higher than the sum of the concentrations of Gamide and Ggly (*15*). Because cleavage of the CTFP from progastrin initially leads to an equivalent amount of Ggly, which may then be converted to Gamide, the greater amount of CTFP provides additional evidence for the generation of fragments of Ggly and/or Gamide. In human gastrinomas, the ratio of the concentration of CTFP to the sum of the concentrations of Gamide and Ggly may be as high as 18-fold (*15*).

We reported recently that Ggly specifically bound two trivalent ferric ions (*16*). The ferric ion ligands were clearly identified as Glu7−Glu9 by NMR spectroscopy. Thus, addition of the first ferric ion broadened beyond detection the resonances from Glu7, and addition of the second ferric ion broadened beyond detection the resonances from Glu8 and Glu9 (*17*). The identification was confirmed by examination of mutant peptides in which one or more of the glutamates were replaced by Ala. Mutation of Glu7 or of Glu8 and Glu9, resulted in a reduction in the stoichiometry of ferric ion binding from two to one, as measured by fluorescence spectroscopy (*17*). Mutation of Glu6 had no effect on the stoichiometry of ferric ion binding.

Binding of ferric ions was essential for the biological activity of Ggly (*17*). Replacement of Glu7 by Ala completely abolished the activity of Ggly in both cell-proliferation and migration assays (*17*), while replacement of Glu6 was without effect. The absolute requirement for ferric ions was confirmed by the observation that the chelating agent desferrioxamine also completely inhibited Ggly activity (*17*). In contrast, studies with the corresponding Glu7Ala mutant of Gamide demonstrated that ferric ions were not essential for binding of Gamide to the CCK-2 receptor or for the biological activity of Gamide (*18*). The importance of ferric ions for the biological activity of Ggly was further demonstrated by our observation that trivalent bismuth ions competed with ferric ions and hence selectively inhibited Ggly activity but had little effect on the actions of Gamide (*19*).

Previous structure−function studies with Ala-substituted Ggly mutants indicated that some of the five consecutive glutamates (Figure 1) were essential for biological activity of Ggly (*17*). The observation that Ggly5−18 was fully active but that Ggly1−11 possessed only partial activity further suggested that the N-terminal tetrapeptide was not essential but that the C-terminal heptapeptide contributed to activity (*17*). To define the minimum biologically active fragment of Ggly, we have extended our structure−function studies on the molecule to determine the relationship between peptide structure, ferric ion binding, and biological activity. The activity of fragments of Ggly has been measured in proliferation and wound-healing assays with the nontransformed gastric epithelial cell line IMGE-5. The requirement for ferric ions for activity was tested by inclusion of the iron chelator desferrioxamine (DFO) in the assays. The stoichiometry of ferric ion binding to the Ggly fragments was determined by absorption spectroscopy, and the residues involved in binding and the affinity of binding were defined by nuclear magnetic resonance (NMR) spectroscopy.

MATERIALS AND METHODS

Chemicals and Cell Lines. Ggly (Ggly1−18, ZGPWLE_5AYGWMDFG) and Ggly fragments (Figure 1) were purchased from Auspep (Melbourne, Australia). The identity of all peptides was confirmed by mass spectral analysis. The purities of the peptides, as assessed by HPLC, were Ggly, 92%; LE_5AYG, 96%; LE_5AY, 98%; E_5AY, 97%; LE_5A, 96%; LE_5, 97%; E_5A, 95%; and E_5, 98%. The impurities consisted of water and salts.

The IMGE-5 cell line was established from the gastric mucosa of mice transgenic for a temperature-sensitive mutant of the SV40 large T antigen as described previously (*20*). IMGE-5 cells were generally grown at 33 °C in Dulbecco's modified Eagle's medium (DMEM) containing 1 unit/mL γ-interferon, 10% fetal bovine serum (FBS), 100 units/mL penicillin, and 100 μg/mL streptomycin (permissive conditions). For all experiments, cells were transferred to the same medium without γ-interferon at 39 °C (nonpermissive conditions), at which temperature they display differentiated characteristics such as expression of functional adherens and tight junctions. All experiments have been performed on cells between passages 20 and 30.

Proliferation Assay. Cell proliferation was assayed by ^{3}H-thymidine incorporation. IMGE-5 cells were seeded in a 96-well plate at a density of $(3-5) \times 10^3$ cells/well in DMEM containing 10% FBS and cultured at 33 °C. On the following day, the cells were serum-starved at 33 °C for 24 h. The cells were then treated with full-length or truncated Ggly at the concentrations indicated in the text, ±1 μM DFO in DMEM containing 1% FBS and 10 μCi/mL [methyl-^{3}H]-thymidine. The cells were cultured at 39 °C for 24 h and then harvested using a NUNC cell harvester. The amount of ^{3}H-thymidine incorporated through DNA synthesis was detected with a β counter (Packard, Meriden, CT).

The effective dose required for 50% stimulation, ED_{50}, and the maximum percent stimulation, *S*, were then obtained, using SigmaPlot (Jandel Scientific, San Rafael, CA), by nonlinear regression of the data to the equation

$$s = 100 + SC/(ED_{50} + C)$$

where *S* is the percent stimulation at a total concentration of Ggly or Ggly fragment, *C*.

Migration Experiments. To assess the effects of Ggly fragments on cell migration, wound-healing experiments were performed as detailed elsewhere (*6*). In brief, IMGE-5 cells were grown in 12-well plates in DMEM at 33 °C until they reached 80% confluence and then shifted to 39 °C and serum starved for 24 h. After the confluent monolayer had been wounded with a 20-μL pipet tip, cells were washed 3 times with phosphate-buffered saline (PBS; 2.7 mM KCl, 1.5 mM KH_2PO_4, 142 mM NaCl, and 10 mM Na_2HPO_4 at pH 6.9) and treated with or without different compounds in DMEM. Morphology and migration of cells were observed and photographed immediately and after treatment for 24 h.

The wound size was measured at six different positions on the photographs, and averages were calculated.

NMR Spectroscopy. The peptides LE_5AYG, LE_5A, E_5AY, and E_5A (approximately 2 mM) were dissolved in H_2O with 5 or 10% ^2H_2O. LE_5AY was only slightly soluble at 2 mM but dissolved completely on addition of $^2H_6$-DMSO (75% H_2O/8% ^2H_2O/17% $^2H_6$-DMSO). The pH was adjusted to 5.3 with $NaO^2H/^2HCl$. ^1H NMR spectra were recorded at 278 K on Bruker AMX 500, Avance 500, or Avance 600 spectrometers as described previously (*17*) and referenced to 2,2-dimethyl-2-silapentane-5-sulfonate at 0 ppm via the chemical shift of the H_2O resonance at 5.00 ppm (4.96 ppm for the 17% $^2H_6$-DMSO samples) (*21*). Sequence-specific ^1H NMR resonance assignments were made from two-dimensional nuclear Overhauser enhancement spectroscopy (NOESY) and total correlation spectroscopy (TOCSY).

Ferric ion titration experiments were carried out by addition of 20, 50, or 200 mM ferric citrate or 100 mM ferric chloride to the peptides. The pH was maintained at 5.3 by addition of small amounts of NaO^2H or ^2HCl. Concentration, pH, temperature, and use of ferric citrate were in keeping with the conditions that were employed in earlier Ggly NMR experiments to prevent precipitation of peptide or ferric hydroxide (*17*). The values of the apparent dissociation constant, K_d, for the complexes between ferric ions and the nonapeptide LE_5AYG or the octapeptide LE_5AY were obtained from the change in chemical shift of the Glu10 amide proton on addition of ferric ions using SigmaPlot, by linear regression of the data to the equation

$$1/\Delta\delta = (K_d/\Delta\delta_{max})(1/[Fe^{3+}]) + (1/\Delta\delta_{max})$$

where $\Delta\delta$ is the change in chemical shift, $\Delta\delta_{max}$ is the maximum change in chemical shift, and $[Fe^{3+}]$ is the concentration of added ferric ions.

Absorption Spectroscopy. Absorption spectra of peptides (100 μM in 5% DMSO/95% 10 mM sodium acetate (pH 4.0) containing 100 mM NaCl and 0.005% Tween 20) in the presence of increasing concentrations of ferric ions were measured against a buffer blank, in 1-mL quartz cuvettes thermostated at 25 °C, with a Cary 5 spectrophotometer (Varian, Mulgrave, Australia).

Statistics. Results are expressed as the means ± standard error of the mean (SEM). Data were analyzed by one-way analysis of variance. If there was a statistically significant difference in the data set, individual values were compared with the appropriate value without DFO by Bonferroni's *t* test. Differences with p values < 0.05 were considered significant.

RESULTS

We have previously utilized quenching of tryptophan fluorescence to show that the 18-residue peptide hormone Ggly (Ggly1−18, $ZGPWLE_5AYGWMDFG$) bound two trivalent ferric ions in aqueous solution (*16*). Examination of the structure of Ggly by ^1H NMR spectroscopy indicated that the first ferric ion bound to Glu7 and the second ferric ion to Glu8 and Glu9 (*17*). The importance of ferric ion binding for biological activity was demonstrated by inclusion of the chelating agent DFO in cell-proliferation and migration assays (*17*). Similar techniques have now been used to investigate the biological activity of Ggly fragments based on the nonapeptide Ggly5−13 (LE_5AYG) (Figure 1) and the ability of such fragments to bind ferric ions. As pointed out in our earlier study of Ggly (*16*), investigation of the complexes between gastrin-derived peptides and ferric ions is hampered by concentration-dependent precipitation of the peptides at pH values below 5.5 and precipitation of iron hydroxides at pH values above 4.0. In this investigation, we also noted that addition of ferric chloride to the Ggly fragments at the millimolar concentrations employed in NMR studies resulted in quantitative precipitation of the peptides from solution. We therefore restricted our studies to the conditions used previously to allow a direct comparison with previous data for Ggly (*16*, *17*); the pH values were 5.3 for NMR experiments, with iron added as ferric citrate, and 4.0 for absorption spectroscopy, with iron added as ferric chloride.

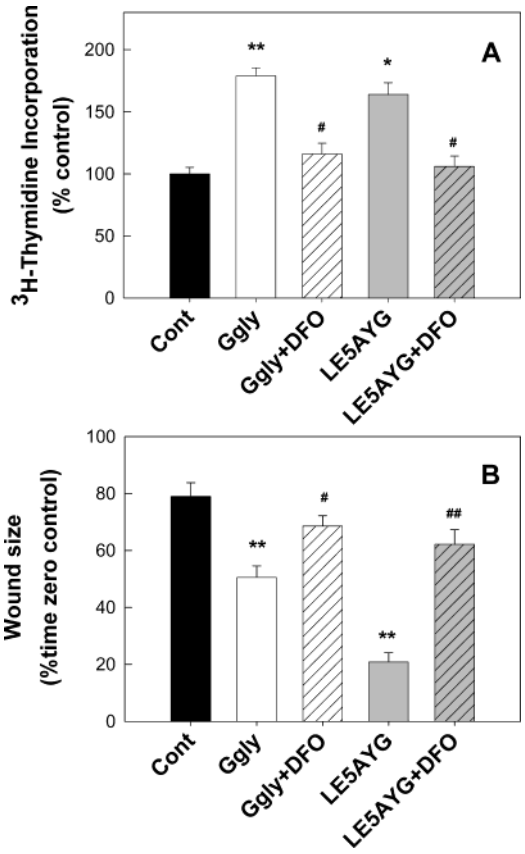

FIGURE 2: Activity of LE_5AYG. The effect of Ggly1−18 (white bars) or the nonapeptide LE_5AYG (gray bars, Ggly5−13, 100 nM, Auspep) on proliferation (A) or migration (B) of IMGE cells was measured as described in the Materials and Methods in thymidine uptake (A) or wound-healing (B) assays, in the absence or presence of the iron chelator DFO (hatched bars). Wound size was measured at time zero and after 24-h treatment. Data are the means ± SEM of two independent experiments, each in triplicate. Statistical significance relative to the control (*, $p < 0.05$; **, $p < 0.01$) or to the peptide-stimulated sample (#, $p < 0.05$; ##, $p < 0.01$) was assessed by one-way analysis of variance, followed by Bonferroni's *t* test.

Activity of the Nonapeptide LE_5AYG. We first compared the activity of Ggly and the nonapeptide LE_5AYG in cell-proliferation and migration assays. The nonapeptide significantly stimulated proliferation of the nontransformed gastric cell line IMGE, as assessed by incorporation of [^{3}H]thymidine, and the stimulation was completely blocked by inclusion of the chelating agent DFO (Figure 2A). In wound-

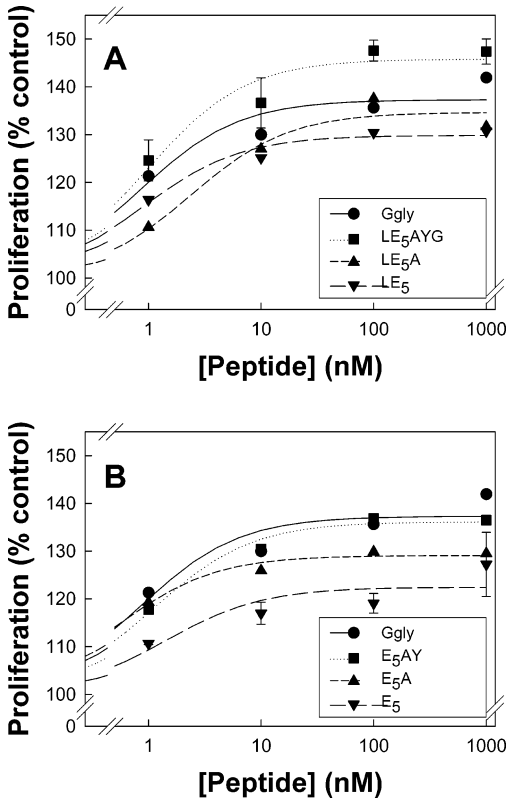

FIGURE 3: Potency of Ggly fragments depends on the chain length. The effects of increasing concentrations of Ggly1−18 (●) or of the indicated fragments of the nonapeptide LE_5AYG (A) or the heptapeptide E_5AY (B) on proliferation of IMGE cells were measured in thymidine uptake assays as described in the Materials and Methods. Points represent the means of five independent experiments, each in duplicate. Lines of best fit to the equation $s = 100 + SC/(ED_{50} + C)$ were generated with Sigmaplot as described in the Materials and Methods. SEM bars are only shown on the maximum and minimum data sets for clarity. The best fit values for ED_{50} and the maximum percent stimulation S used to construct the lines are presented in Table 1.

healing assays, the nonapeptide appeared to be more effective than Ggly in stimulating cell migration (Figure 2B). Again, the stimulation of migration by the nonapeptide LE_5AYG was reversed by inclusion of DFO in the medium.

Activity of Shorter Ggly Fragments. We then investigated the activity of shorter fragments of Ggly in cell-proliferation assays. All fragments stimulated proliferation of IMGE cells in a dose-dependent manner (Figure 3), but curve fitting of the experimental data indicated that the maximum stimulation achieved at saturating concentrations of the hexapeptides LE_5 and E_5A and the pentapeptide E_5 was significantly less than that achieved with the nonapeptide LE_5AYG (Table 1). In contrast, no significant difference was observed between the maximum stimulation achieved at saturating concentrations of the heptapeptides LE_5A and E_5AY and the nonapeptide LE_5AYG. The fact that there was no significant difference between the ED_{50} values observed for any of the peptides (Table 1) suggested that all peptides bound to the Ggly receptor with similar affinities to the nonapeptide LE_5AYG.

Dependence of Activity on Ferric Ions. To determine whether the biological activity of Ggly fragments required ferric ions, we next investigated the effect of DFO on cell proliferation induced by the Ggly fragments. The activities of the nonapeptide LE_5AYG and the heptapeptide E_5AY were

Table 1: Affinity and Potency of Ggly and Ggly Fragments as Stimulants of Cell Proliferation[a]

peptide	ED_{50} (nM)	SEM (nM)	repli-cates	S (%)	SEM	repli-cates	signifi-cance
Ggly	0.8	0.4	5	37.3	2.4	5	NS
LE_5AYG	1.0	0.4	5	45.8	2.5	5	
LE_5A	2.4	1.1	5	34.7	2.6	5	NS
LE_5	0.9	0.7	5	29.9	3.5	5	0.003
E_5AY	1.1	0.7	5	36.1	3.4	5	NS
E_5A	0.5	0.4	5	29.1	3.1	5	0.002
E_5	1.4	1.0	5	22.5	2.5	5	<0.001

[a] Effects of increasing concentrations of Ggly1−18 or of Ggly fragments on the proliferation of IMGE cells were measured in thymidine uptake assays as described in the Materials and Methods. The data from five independent experiments (Figure 3) were fitted to the equation $s = 100 + SC/(ED_{50} + C)$ with Sigmaplot as described in the Materials and Methods, to obtain the indicated values (and SEM) for ED_{50} and the maximum percent stimulation S indicated above. The significance of the differences in the S values from the value for the nonapeptide LE_5AYG was assessed by one way analysis of variance, followed by Bonferroni's t test. There was no significant difference in the ED_{50} values.

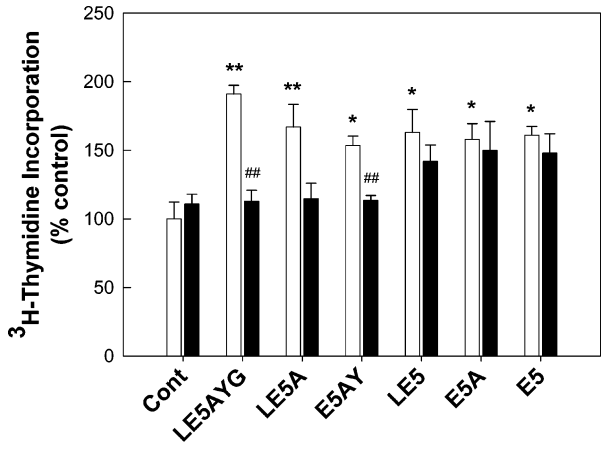

FIGURE 4: Dependence of activity on ferric ions. The effect of Ggly fragments (100 nM) on proliferation of IMGE cells was measured in thymidine uptake assays as described in the Materials and Methods, in the absence (black bars) or presence (gray bars) of the iron chelator DFO. Data are the means ± SEM of at least three independent experiments, each in duplicate. Statistical significance relative to the unstimulated control (*, $p < 0.05$; **, $p < 0.01$) was assessed by one-way analysis of variance, followed by Bonferroni's t test. Statistical significance of each peptide with DFO relative to the corresponding treatment without DFO (##, $p < 0.01$) was determined by a t test. While the activity of Ggly fragments of seven residues or more was inhibited by DFO, the activity of shorter fragments was not dependent on ferric ions.

significantly blocked by DFO in [^{3}H]thymidine incorporation assays (Figure 4). The activity of the heptapeptide LE_5A appeared to be lower in the presence of DFO, although the reduction did not reach significance ($p = 0.059$). However, no significant reduction of the activity of the hexapeptides LE_5 or E_5A or the pentapeptide E_5 was observed in the presence of DFO (Figure 4).

Peptide Structures. We next investigated the structure of the nonapeptide LE_5AYG and shorter Ggly fragments in aqueous solution by NMR spectroscopy. ^{1}H chemical shifts and NH−C$^\alpha$H coupling constants determined from 1D, TOCSY and NOESY spectra of the nonapeptide LE_5AYG in 95% H_2O/5% ^2H_2O at pH 5.3 and 278 K are given in Supplementary Table S1 of the Supporting Information. In

contrast to the well-defined structure observed for Ggly in solution, the nonapeptide LE_5AYG appeared to be unstructured. That is, nuclear Overhauser enhancements were only observed between resonances from the same or neighboring residues; NH and $C^{\alpha}H$ chemical shifts (with the exception of the C-terminal NH resonance) did not differ from random coil values (*22*) by more than 0.3 ppm; and NH−$C^{\alpha}H$ coupling constants ranged from 6 to 8 Hz. These features are consistent with conformational averaging of the peptide backbone. The loss of structure on deletion of residues 14−18 of Ggly is in agreement with our previous suggestion that the disklike structure of Ggly is stabilized by hydrophobic interactions involving Trp14 and Phe17 (*17*).

Similar results were obtained with shorter Ggly fragments. ^1H chemical shifts and NH−$C^{\alpha}H$ coupling constants determined from 1D, TOCSY and NOESY spectra of LE_5AY, LE_5A, E_5AY, and E_5 in 90% H_2O/10%D_2O at pH 5.3 and 278 K are given in Supplementary Tables S2−S5 of the Supporting Information, respectively. For the octapeptide LE_5AY, it was necessary to add $^2H_6$-DMSO to 17% to dissolve the sample, and some of the differences in the positions of individual resonances may therefore be the result of the addition of DMSO. As with the nonapeptide LE_5AYG, the shorter fragments also lack a well-defined structure in aqueous solution.

Definition of Ferric Ion Ligands. To define the ligands involved in ferric ion binding, we next investigated the effect of ferric ions on the NMR spectra of the nonapeptide LE_5AYG. Addition of paramagnetic ferric ions as ferric chloride resulted in quantitative precipitation of the nonapeptide from solution. On addition of ferric citrate (1:1), changes were observed in the line widths, resolution, and chemical shifts of the NH resonances of the nonapeptide LE_5AYG. In contrast to Ggly, where addition of the first ferric ion broadened beyond detection the resonances from Glu7 and addition of the second ferric ion broadened beyond detection the resonances from Glu8 and Glu9 (*17*), the largest effects were observed for the overlapping NH peaks of the Glu9 and Glu10 residues (numbering as for the parent Ggly) (Figure 5A and Supplementary Table S6 of the Supporting Information). The maximum change in chemical shift observed was 0.06 ppm at 2 mol of added Fe^{3+}/mol of peptide for Glu10. At 5 mol of Fe^{3+}/mol, there was a general degradation in the spectral quality because of the high concentration of paramagnetic ions in solution, but the peaks had returned to within 0.01 ppm of their original chemical-shift values. A downfield shift was likewise seen in the multiplet consisting of the overlapping $C^{\gamma}H$ resonances of the Glu6−Glu10 side chains, which has a maximum at 2.32 ppm. When these effects are closer to the site of ferric ion binding, they are larger than those on the corresponding NH resonances, but overlap of the triplets made the effect on each specific residue more difficult to observe. At 2 mol of Fe^{3+}/mol, two unresolved maxima could be discerned in the broadened multiplet, 0.11 and 0.19 ppm downfield from the maximum observed in the absence of ferric ions. At 5 mol of Fe^{3+}/mol, the peak had returned to 2.34 ppm. A TOCSY spectrum of the peptide with 2 mol of Fe^{3+}/mol confirmed that the Glu9 and Glu10 $C^{\gamma}H$ resonances at 2.31 and 2.28 ppm, respectively, in the ferric ion-free sample, were most affected. The glutamate $C^{\beta}H$ multiplet moved downfield by 0.02 ppm. Other side-chain chemical shifts were unaffected

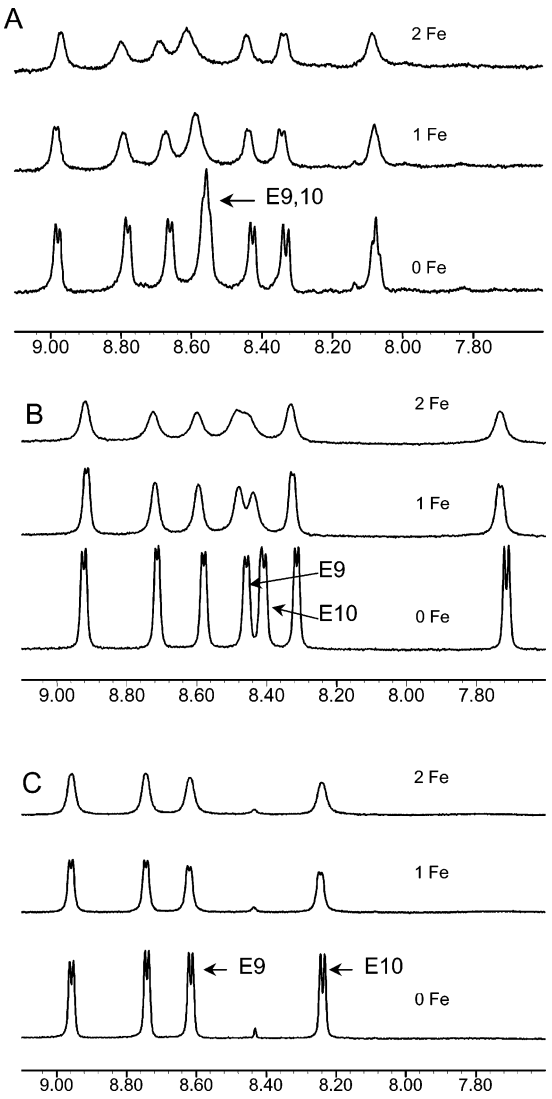

FIGURE 5: Definition of ferric ion ligands. The amide region of the one-dimensional ^1H NMR spectrum of LE_5AYG (A) at 500 MHz or LE_5AY (B) or E_5 (C) at 600 MHz are shown. Peptide concentrations were approximately 2 mM in 95% H_2O/5% ^2H_2O (A), 75% H_2O/8% ^2H_2O/17% $^2H_6$-DMSO (B), or 90% H_2O/10% ^2H_2O (C) at pH 5.3. The N-terminal amino group is not visible from fast exchange; the remaining resonances are fortuitously in the same order as the peptide sequences. Addition of 1 or 2 mol/mol of ferric citrate to the nonapeptide LE_5AYG or the octapeptide LE_5AY caused a selective downfield shift in the resonances because of Glu9 and Glu10 (arrows, numbering as for Ggly). The observation that the Glu9 and Glu10 NH resonances showed the largest downfield shifts was reproducible with different batches of peptides, but the magnitudes of the ferric-ion-induced shifts differed slightly between experiments. Addition of ferric citrate to the pentapeptide E_5 did not shift the glutamate resonances. Note that some of the differences in the positions of individual resonances may be the result of the different DMSO concentrations.

by addition of Fe^{3+}, except for the terminal Gly $C^{\alpha}H$ resonance, which moved downfield by 0.05 ppm, probably because of the interaction of the terminal acid group with ferric ions. The observation that the Glu9 and Glu10 NH resonances showed the largest downfield shifts was reproducible with different batches of peptide, although the magnitudes of the ferric-ion-induced shifts differed slightly between experiments. Because no ferric-ion-induced changes in chemical shift were observed when EDTA was added to the nonapeptide before ferric citrate (spectra not shown), we

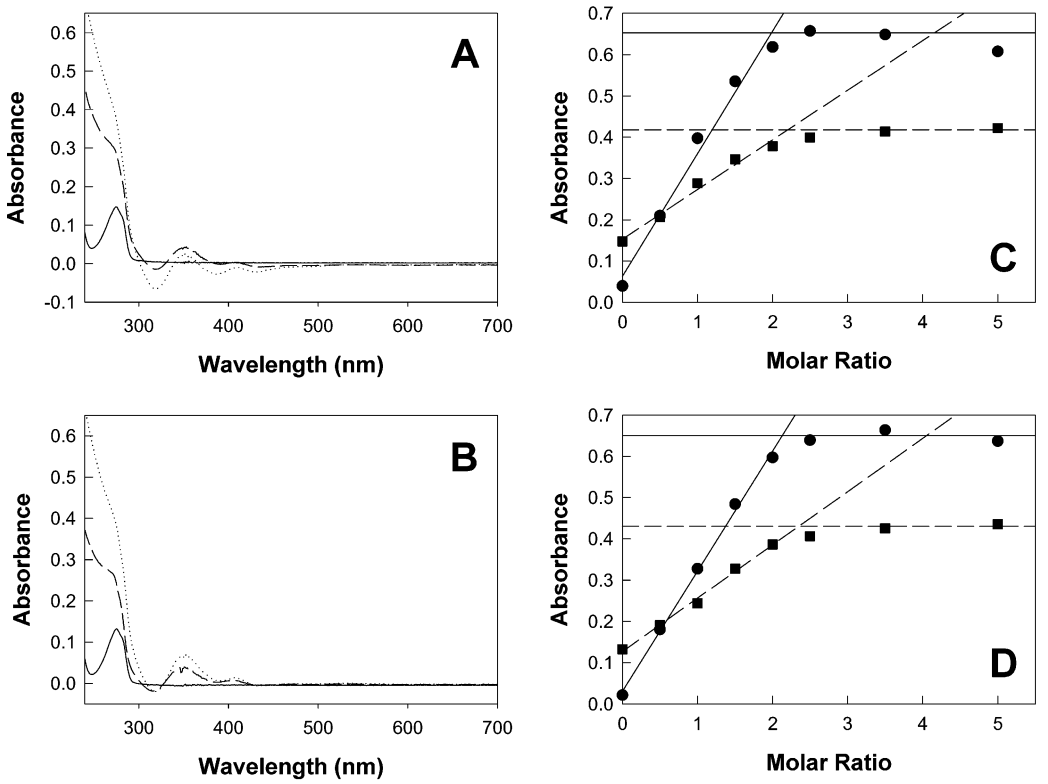

FIGURE 6: Stoichiometry of ferric ion binding. The absorption spectrum of (A) the nonapeptide LE_5AYG or (B) the heptapeptide E_5AY (100 μM in 5% DMSO/95% 10 mM sodium acetate (pH 4.0) containing 100 mM NaCl and 0.005% Tween 20) in the absence (—) and presence of ferric ions at a ratio of 1 (- - -) or 2 (···) mol/mol was measured at 25 °C in a Cary 5 spectrophotometer as described in the Materials and Methods. The spectrum was corrected for the change observed when the same concentration of ferric ions was added to 5% DMSO in the buffer alone. Addition of aliquots of ferric chloride to (C) the nonapeptide or (D) the heptapeptide resulted in a linear increase in the absorption minimum at 247 nm up to a molar ratio of approximately 2 (●). A similar stoichiometry was observed from titrations at the absorption maximum of 275 nm (■). The mean values for stoichiometry and maximum increase for the three tyrosine-containing peptides LE_5AYG, LE_5AY, and E_5AY from three independent experiments are presented in Table 2.

conclude that all changes were dependent on ferric ion binding to the nonapeptide.

We then investigated the effect of added ferric ions on the NMR spectra of shorter Ggly fragments. Addition of ferric ions as ferric citrate to the octapeptide LE_5AY again resulted in a downfield shift in the NH resonances from Glu9 and Glu10, with a maximum change in chemical shift of 0.05 ppm at 2 mol of added Fe^{3+}/mol of peptide (Figure 5B and Supplementary Table S6 of the Supporting Information). The maximum for the overlapping C$^\gamma$H resonances had again diverged into two maxima 0.11 and 0.12 ppm downfield, the latter movement being 0.07 ppm smaller than the movement for LE_5AYG. For the heptapeptides LE_5A and E_5AY, smaller downfield shifts were observed in the NH resonances from Glu9 and Glu10, with a maximum change in chemical shift of 0.01 ppm at 2 mol of added Fe^{3+}/mol of peptide (Supplementary Table S6 of the Supporting Information). For the pentapeptide E_5, no shift was observed in the NH resonances from either Glu9 or Glu10 (Figure 5C and Supplementary Table S6 of the Supporting Information). Thus, the evidence is clear-cut that, in contrast to Ggly, which binds ferric ions via Glu7−Glu9 (*17*), the nonapeptide LE_5AYG and the octapeptide LE_5AY bind ferric ions via Glu9 and Glu10. The data with the heptapeptides LE_5A and E_5AY are consistent with the same conclusion, although the binding in this case is weaker. In fact, the decrease in the magnitude of the maximum change in chemical shift from the nonapeptide to the pentapeptide supports the generalization that the affinity of the peptides for ferric ions decreases with decreasing chain length.

Table 2: Stoichiometry of Ferric Ion Binding by Ggly and Ggly Fragments[a]

peptide	stiochiometry	SEM	fold increase	SEM	replicates
Ggly	2.0[b]	0.3[b]	2.1[b]	0.3[b]	3[b]
LE_5AYG	1.93	0.15	2.0	0.4	3
LE_5AY	2.15	0.03	2.9	0.1	3
E_5AY	2.58	0.03	3.5	0.1	3

[a] Stoichiometry of ferric ion binding to Ggly fragments containing tyrosine residues and the maximum increase in absorbance on addition of ferric ions were determined at the absorption maximum of 275 nm as described in the caption of Figure 6. Values from the indicated number of independent experiments were combined to obtain the mean values (±SEM) presented above. [b] Values taken from ref *16*.

Stoichiometry of Ferric Ion Binding to Ggly Fragments. The stoichiometry of ferric ion binding to Ggly fragments containing tyrosine residues was measured by absorbance spectroscopy (*16*). The ultraviolet absorbance of both the nonapeptide LE_5AYG (Figure 6A) and the heptapeptide E_5AY (Figure 6B) increased markedly on addition of ferric ions. Titration experiments at either the absorbance minimum at 247 nm or the absorbance maximum at 275 nm revealed that for both the nonapeptide LE_5AYG (Figure 6C) and the heptapeptide E_5AY (Figure 6D) the stoichiometry of binding was approximately 2 mol of ferric ion per mol of peptide (Table 2). Similar results were obtained with the octapeptide LE_5AY (data not shown). The increase in absorbance at the

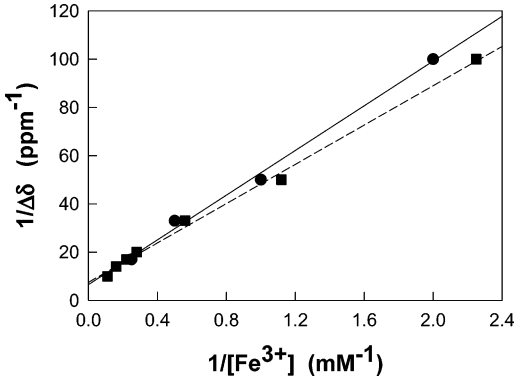

FIGURE 7: Affinity of ferric ion binding. The reciprocal of the change in chemical shift ($\Delta\delta$) of the Glu10 NH resonance of the nonapeptide LE_5AYG (●) or the octapeptide LE_5AY (■) was plotted against the reciprocal of the concentration of added ferric citrate ($[Fe^{3+}]$) as described in the Materials and Methods. Lines of best fit were obtained by linear regression with Sigmaplot, and values of the apparent dissociation constant K_d (LE_5AYG, 7.0 mM, $r^2 = 0.995$; LE_5AY, 5.4 mM, $r^2 = 0.996$) were calculated by dividing the slope by the ordinate intercept.

absorbance maximum at 275 nm (2−3.6-fold) was similar to the 2.1-fold increase previously observed at the absorbance maximum at 281 nm on addition of ferric ions to Ggly. The increase in absorbance at the absorbance minimum at 247 nm (LE_5AYG, 7.1 ± 1.6-fold; LE_5AY, 12 ± 1-fold; and E_5AY, 17 ± 2-fold) was much greater than the 3.3-fold increase previously observed at the absorbance minimum at 250 nm on addition of ferric ions to Ggly.

Affinity of Ferric Ion Binding to Ggly Fragments. The affinity of Ggly for ferric ions was originally measured by quenching of the fluorescence of the two tryptophan residues (*16*). The binding data were well-fitted by a model with two equivalent but independent binding sites (*16*). The same approach could not be used in the present study because the Ggly fragments lack tryptophan. However, the affinity of the Ggly fragments for ferric ions could be measured from the shift in the Glu10 amide resonance on addition of ferric ions (Figure 7). The apparent K_d values of 7.0 mM obtained for the nonapeptide LE_5AYG and 5.4 mM for the octapeptide LE_5AY are considerably weaker than the K_d value of 0.6 μM obtained previously for Ggly in fluorescence experiments. Furthermore, the reduction observed from the nonapeptide to the pentapeptide in the magnitude of the maximum change in chemical shift on addition of ferric ions is consistent with the suggestion that the affinity of peptides shorter than the nonapeptide for ferric ions decreases with a decreasing chain length. However, the reduction in the maximal chemical shift prevented accurate estimation of K_d values for shorter Ggly fragments.

DISCUSSION

Previous studies with Ggly fragments revealed that either the N or C terminal could be deleted without complete loss of biological activity (*17*, *23*). Thus, the peptide LE_5-AYGWMDFG, formed by removal of the four N-terminal residues of Ggly, was fully active in cell-proliferation or wound-healing assays, while the activity of the peptide $ZGPWLE_5A$, formed by removal of the seven C-terminal residues, was reduced by approximately 50% (*17*). Similarly, both Ggly1−13 ($ZGPWLE_5AYG$) and Ggly6−18 (E_5AYG-WMDFG) were biologically active in stimulating gene expression in canine gastric parietal cells (*23*). The results presented herein reveal that simultaneous deletion of both four N-terminal and five C-terminal residues to form the nonapeptide LE_5AYG has no effect on maximal activity in either proliferation or migration assays (Figure 2) or on potency in proliferation assays (Table 1). These observations are in sharp contrast to the structure−function profile of amidated gastrins, in which only the four C-terminal residues are essential for activity (*24*).

As a result of multiple post-translational processing steps, the gastric antrum contains a heterogeneous mixture of large progastrin-derived peptides and shorter fragments of Gamide such as amidated gastrin2−17, 4−17, 6−17, and 13−17 (*13*, *14*). Many of these processing products are also found in the circulation. Equivalent forms derived from Ggly have not yet been isolated from the human antrum, although substantial amounts of gastrin2−17gly are present in the rat antrum (*25*). N-terminal fragments, particularly gastrin1−10, are present in the human antrum in concentrations equivalent to Gamide (*14*). The presence of gastrin1−10 is relevant to the present study because the processing site Glu10-Ala11 follows the pentaglutamate sequence. A combination of the Glu10-Ala11 bond cleavage with the Leu5-Glu6 bond cleavage that generated gastrin6−17 would produce the pentapeptide E_5. Similarly, a combination of the Leu5-Glu6 bond cleavage that generated gastrin6−17 with the Tyr12-Gly13 bond cleavage that generated gastrin13−17 would produce the heptapeptide E_5AY. However, direct demonstration of the gastrin nonapeptide LE_5AYG and its smaller fragments in human antrum and serum and measurement of their concentration in the circulation by radioimmunoassay will be dependent on the development of new antibodies, because current radioimmunoassays are directed at either the N or C termini of Gamide and Ggly.

The biological activity of the nonapeptide LE_5AYG is still absolutely dependent on the presence of ferric ions. As with Ggly (*17*), activity in both proliferation and migration assays is completely blocked by inclusion of the chelating agent DFO in the medium. Absorbance spectroscopy indicated that the nonapeptide still bound 2 ferric ions (Figure 6), although the affinity of ferric ions for the nonapeptide (apparent $K_d = 7.0$ mM at pH 5.3) as determined from NMR experiments (Figure 7) was much lower than the affinity previously calculated for Ggly from fluorescence experiments [$K_d = 0.6$ μM at pH 4.0 (*16*)]. At least part of the difference is the result of the inclusion of citrate in the NMR experiments to increase ferric ion solubility at the higher pH. Attempts to repeat the LE_5AYG titration with ferric chloride instead of ferric citrate resulted in the immediate formation of a precipitate and a quantitative reduction in the intensity of the signal from the peptide remaining in solution. These observations suggest that ferric ions bind strongly to the peptide but that, when citrate is present, the apparent K_d is reduced by competition with the citrate.

The affinities of Ggly and gastrin fragments for ferric ions were measured at acidic pH values to circumvent problems with precipitation of iron hydroxides (*16*). The affinities at neutral pH are presumably considerably higher but could not be calculated because precipitation of Ggly and Gamide at acidic pH values has prevented measurement of the pK_a values of all of their glutamate residues (*16*). We are

therefore unable to calculate the fractional occupancy of the ferric-ion-binding sites of Ggly and gastrin fragments under physiological conditions. However, the experimental observation that the chelating agent DFO completely blocks the activity of Ggly and LE_5AYG in proliferation and migration assays (Figure 2) clearly establishes that ferric ion binding occurs and is critically important in tissue culture experiments at neutral pH.

Determination of the affinities of Ggly and the nonapeptide for ferric ions by the same method is not possible at present. We could not estimate the affinity of the nonapeptide and shorter Ggly fragments by fluorescence spectroscopy as we had previously with Ggly, because the nonapeptide lacks tryptophan. We also could not determine the apparent affinity of ferric ions for Ggly from our previous NMR experiments because the stoichiometric reduction in the Glu7−Glu9 resonances on addition of ferric ions made the monitoring of chemical-shift changes difficult (*17*). However, the different behavior of the amide proton resonances of Ggly and Ggly fragments on addition of ferric ions, with the Glu9 and Glu10 resonances of the nonapeptide and octapeptide shifting downfield (parts A and B of Figure 5) and the Glu7−Glu9 resonances of Ggly stoichiometrically reduced, is consistent with the observed considerable difference in affinity between the two peptides.

Part of the reduction in affinity for ferric ions between Ggly and the nonapeptide and octapeptide may be the result of the participation of different glutamates as ferric ion ligands. Thus, for Ggly, the first ferric ion binds to Glu7 and the second to Glu8 and Glu9 (*17*), while for the nonapeptide and octapeptide, the observation that binding of ferric ions simultaneously affects Glu9 and Glu10 (numbering as for the parent Ggly) suggests that these two residues act as ligands at both the first and second ion-binding sites. The change in iron ligation may in turn result from the loss of the well-defined loop in the Ggly structure (*17*) consequent on removal of the hydrophobic residues Trp14 and Phe17 (Figure 1).

Ggly fragments shorter than the nonapeptide are also biologically active, but the dependence on ferric ions varies with the chain length. The shortest fully active fragments of Ggly are the heptapeptides LE_5A and E_5AY (Table 1), for both of which activity remains iron-dependent (Figure 4). Further N- or C-terminal truncation results in a progressive reduction in maximal activity, although there is no significant change in potency (Table 1). Interestingly, the hexapeptides LE_5 and E_5A and the pentapeptide E_5 possess significant activity (Table 1), which is not reduced in the presence of the chelating agent DFO (Figure 4). In the NMR experiments, the reduction observed from the nonapeptide to the pentapeptide in the magnitude of the maximum change in the chemical shift on addition of ferric ions (Supplementary Table S6 of the Supporting Information) is consistent with the suggestion that the affinity of the shorter peptides for ferric ions decreases with a decreasing chain length. The failure of DFO to inhibit the activity of the Ggly fragments LE_5, E_5A, or E_5 (Figure 4) is presumably therefore a reflection of the reduced affinity of the shorter peptides for ferric ions. The observation that the fragments LE_5, E_5A, or E_5 possess significant ferric ion-independent activity is unexpected and will be the subject of further investigation.

This study has several important implications. The observation that fragments as short as the heptapeptides LE_5A and E_5AY are fully active indicates that extensive proteolytic processing may not completely inactivate Ggly and that bioactive forms that are not detected by current radioimmunoassays may be present in tissues and/or plasma. Our results with the nonapeptide LE_5AYG and the heptapeptides LE_5A and E_5AY confirm the critical role played by ferric ions in the biological activities of Ggly and indicate that iron-selective chelating agents may act as antagonists of the proliferative and migratory effects of Ggly and its longer fragments in vivo. Moreover, the demonstration that the N and C termini of Ggly can be removed without altering biological activity suggests that future attempts to design Ggly antagonists could begin with Ggly fragments as short as the heptapeptides LE_5A or E_5AY.

SUPPORTING INFORMATION AVAILABLE

Chemical shifts and coupling constants for the peptides LE_5AYG, LE_5AY, LE_5A, E_5AY, LE_5, E_5A, and E_5 and chemical-shift changes on addition of ferric ions. This material is available free of charge via the Internet at http://pubs.acs.org.

REFERENCES

1. Dockray, G. J., Varro, A., Dimaline, R., and Wang, T. (2001) The gastrins: Their production and biological activities, *Annu. Rev. Physiol. 63*, 119−139.
2. Dockray, G. J. (1999) Gastrin and gastric epithelial physiology, *J. Physiol. 518*, 315−324.
3. Seva, C., Dickinson, C. J., and Yamada, T. (1994) Growth-promoting effects of glycine-extended progastrin, *Science 265*, 410−412.
4. Hollande, F., Imdahl, A., Mantamadiotis, T., Ciccotosto, G. D., Shulkes, A., and Baldwin, G. S. (1997) Glycine-extended gastrin acts as an autocrine growth factor in a nontransformed colon cell line, *Gastroenterology 113*, 1576−1588.
5. Stepan, V. M., Sawada, M., Todisco, A., and Dickinson, C. J. (1999) Glycine-extended gastrin exerts growth-promoting effects on human colon cancer cells, *Mol. Med. 5*, 147−159.
6. Hollande, F., Choquet, A., Blanc, E. M., Lee, D. J., Bali, J. P., and Baldwin, G. S. (2001) Involvement of phosphatidylinositol 3-kinase and mitogen-activated protein kinases in glycine-extended gastrin-induced dissociation and migration of gastric epithelial cells, *J. Biol. Chem. 276*, 40402−40410.
7. Kermorgant, S., and Lehy, T. (2001) Glycine-extended gastrin promotes the invasiveness of human colon cancer cells, *Biochem. Biophys. Res. Commun. 285*, 136−141.
8. Koh, T. J., Dockray, G. J., Varro, A., Cahill, R. J., Dangler, C. A., Fox, J. G., and Wang, T. C. (1999) Overexpression of glycine-extended gastrin in transgenic mice results in increased colonic proliferation, *J. Clin. Invest. 103*, 1119−1126.
9. Wang, T. C., Koh, T. J., Varro, A., Cahill, R. J., Dangler, C. A., Fox, J. G., and Dockray, G. J. (1996) Processing and proliferative effects of human progastrin in transgenic mice, *J. Clin. Invest. 98*, 1918−1929.
10. Aly, A., Shulkes, A., and Baldwin, G. S. (2001) ShortOLINIT-term infusion of glycine extended gastrin (17) stimulates both proliferation and formation of aberrant crypt foci in rat colonic mucosa, *Int. J. Cancer 94*, 307−313.
11. Higashide, S., Gomez, G., Greeley, G. H., Jr., Townsend, C. M., Jr., and Thompson, J. C. (1996) Glycine-extended gastrin potentiates gastrin-stimulated gastric acid secretion in rats, *Am. J. Physiol. 270* (Part 1), G220−G224.
12. Chen, D., Zhao, C. M., Dockray, G. J., Varro, A., Van Hoek, A., Sinclair, N. F., Wang, T. C., and Koh, T. J. (2000) Glycine-extended gastrin synergizes with gastrin 17 to stimulate acid secretion in gastrin-deficient mice, *Gastroenterology 119*, 756−765.
13. Rehfeld, J. F. (1998) The new biology of gastrointestinal hormones, *Physiol. Rev. 78*, 1087−1108.

14. Rehfeld, J. F., Hansen, C. P., and Johnsen A. H. (1995). Post-poly(Glu) cleavage and degradation modified by O-sulfated tyrosine: A novel post-translational processing mechanism, *EMBO J. 14*, 389−396.
15. Pauwels, S., Desmond, H., Dimaline, R., and Dockray, G. J. (1986) Identification of progastrin in gastrinomas, antrum, and duodenum by a novel radioimmunoassay, *J. Clin. Invest. 77*, 376−381.
16. Baldwin, G. S., Curtain, C. C., and Sawyer, W. H. (2001) Selective, high-affinity binding of ferric ions by glycine-extended gastrin(17), *Biochemistry 40*, 10741−10746.
17. Pannequin, J., Barnham, K. J., Hollande, F., Shulkes, A., Norton, R. S., and Baldwin, G. S. (2002) Ferric ions are essential for the biological activity of the hormone glycine-extended gastrin, *J. Biol. Chem. 277*, 48602−48609.
18. Pannequin, J., Tantiongco, J.-P., Kovac, S., Shulkes, A., and Baldwin, G. S. (2004) Divergent roles for ferric ions in the biological activity of amidated and non-amidated gastrins, *J. Endocrinol. 181*, 315−325.
19. Pannequin, J., Kovac, S., Tantiongco, J.-P., Norton, R. S., Shulkes, A., Barnham, K. J., and Baldwin, G. S. (2004) A novel effect of bismuth ions. Selective inhibition of the biological activity of glycine-extended gastrin, *J. Biol. Chem. 279*, 2453−2460.
20. Hollande, F., Blanc, E. M., Bali, J. P., Whitehead, R. H., Pelegrin, A., Baldwin, G. S., and Choquet, A. (2001) HGF regulates tight junctions in new nontumorigenic gastric epithelial cell line, *Am. J. Physiol. 280*, G910−G921
21. Wishart, D. S., Bigam, C. G., Yao, J., Abildgaard, F., Dyson, H. J., Oldfield, E., Markley, J. L., and Sykes, B. D. (1995) ^{1}H, ^{13}C, and ^{15}N chemical shift referencing in biomolecular NMR, *J. Biomol. NMR. 6*, 135−140.
22. Merutka, G., Dyson, H. J., and Wright, P. E. (1995*)* "Random coil" ^{1}H chemical shifts obtained as a function of temperature and trifluoroethanol concentration for the peptide series GGXGG, *J. Biomol. NMR 5*, 14−24.
23. Kaise, M., Muraoka, A., Seva, C., Takeda, H., Dickinson, C. J., and Yamada, T. (1995) Glycine-extended progastrin processing intermediates induce H^+,K^+-ATPase α-subunit gene expression through a novel receptor, *J. Biol. Chem. 270*, 11155−11160.
24. Tracy, H. J., and Gregory, R. A. (1964) Physiological properties of a series of synthetic peptides structurally related to gastrin I, *Nature 204*, 935−938.
25. Keire, D. A. Wu, V. S., Diehl, D. L., Chew, P., Ho, F. J., Davis, M. T., Lee, T. D., Shively, J. E., Walsh, J. H., and Reeve, J. R., Jr. (2003) Rat progastrin processing yields peptides with altered potency at the CCK-B receptor, *Regul. Pept. 113*, 115−124.

BI0495984